AD_____

Award Number: DAMD17-02-2-0011

TITLE: Structural Studies on Intact Clostridium Botulinum Neurotoxins Complexed with Inhibitors Leading to Drug Design

PRINCIPAL INVESTIGATOR: Subramanyam Swaminathan, Ph.D.

CONTRACTING ORGANIZATION: Brookhaven National Laboratory
Upton, New York 11973

REPORT DATE: February 2003

TYPE OF REPORT: Annual

PREPARED FOR: U.S. Army Medical Research and Materiel Command
Fort Detrick, Maryland 21702-5012

REPORT DOCUMENTATION PAGE

Form Approved
OMB No. 074-0188

1. AGENCY USE ONLY (Leave blank)	2. REPORT DATE	3. REPORT TYPE AND DATES COVERED
	February 2003	Annual (28 Jan 02 - 27 Jan 03)

4. TITLE AND SUBTITLE
Structural Studies on Intact Clostridium Botulinum Neurotoxins Complexed with Inhibitors Leading to Drug Design

5. FUNDING NUMBERS
DAMD17-02-2-0011

6. AUTHOR(S)
Subramanyam Swaminathan, Ph.D.

7. PERFORMING ORGANIZATION NAME(S) AND ADDRESS(ES)
Brookhaven National Laboratory
Upton, New York 11973

E-Mail: swami@bnl.gov

8. PERFORMING ORGANIZATION REPORT NUMBER

9. SPONSORING / MONITORING AGENCY NAME(S) AND ADDRESS(ES)
U.S. Army Medical Research and Materiel Command
Fort Detrick, Maryland 21702-5012

10. SPONSORING / MONITORING AGENCY REPORT NUMBER

11. SUPPLEMENTARY NOTES
Original contains color plates: All DTIC reproductions will be in black and white.

12a. DISTRIBUTION / AVAILABILITY STATEMENT
Approved for Public Release. Distribution Unlimited.

12b. DISTRIBUTION CODE

13. ABSTRACT (Maximum 200 Words)

In this first annual report we present our progress in three of the Statement of Work. In addition we have included our work being done in collaboration with Walter Reed Army Institute of Research. Structural work with *Clostridium botulinum* B and a potential inhibitor, BABIM, is reported. Though it was predicted that it would bind to the active site, we have shown that it binds at two sites in BoNT/B, the active site and the substrate-binding site. We speculate that the inhibitory property of this molecule may be because it chelates the active site zinc or because it blocks the substrate binding site or due to both. We also propose that analogs of BABIM might work better. We are continuing with our studies on BoNT/B with other potential inhibitors. A set of potential inhibitors identified by biochemical methods and a few small molecules known to inhibit zinc endopeptidases like thermolysin and carboxypeptidase have been screened by computational methods before determining the structures of the complexes. Combining the docking calculations with the x-ray diffraction methods offers a powerful rational design of inhibitors. From our studies so far we conclude that small molecules that will stay bound to the toxins will be the best inhibitors.

14. SUBJECT TERMS
Clostridium, botulinum, neurotoxin, zinc chelators, inhibitors, macromolecular crystallography, 3D structure

15. NUMBER OF PAGES
27

16. PRICE CODE

17. SECURITY CLASSIFICATION OF REPORT	18. SECURITY CLASSIFICATION OF THIS PAGE	19. SECURITY CLASSIFICATION OF ABSTRACT	20. LIMITATION OF ABSTRACT
Unclassified	Unclassified	Unclassified	Unlimited

Table of Contents

Structural Studies on Intact *Clostridium botulinum* Neurotoxins Complexed with Inhibitors Leading to Drug Design
Annual Report for the Period ending January 2003

Introduction

The major goal of this project is to identify small-molecule inhibitors and antidotes to block the activity of botulinum neurotoxins. Though the catalytic activity is confined to the light chain of the whole toxin, the goal of this project is to identify such molecules when the whole intact neurotoxin is considered. The general approach followed here is to determine the three dimensional structures of complexes of botulinum neurotoxin and small molecules or zinc chelators, and to analyze the interaction between the potential inhibitors and the protein and to suggest ways to modify the inhibitor for better binding and more effective inhibition of toxicity. Here, we report progress made on three of the Statement Of Work (SOW) enumerated in our proposal.

Body

(1) Botulinum neurotoxin B in complex with Bis(5-amidinobenzimidazolyl) methane (BABIM)

Crystals of *Clostridium botulinum* neurotoxin B were soaked in a mother liquor containing the well known zinc chelator bis(5-amidino-2-benzimidazolyl)methane (BABIM). Initially various concentrations of BABIM and durations of soaking were tried to test the stability of the crystal and its diffraction quality in order to find the optimum conditions of soaking. The optimum concentration of the inhibitor was determined to be 3 mM. Higher concentrations of BABIM even with a very short soaking time either destroyed the crystal or caused poor diffraction quality. Since the goal was to study the inhibition mechanism, it was decided to stop the inhibition reaction after soaking the crystal for various durations of time by plunging the soaked crystal in liquid nitrogen. Four durations of soaking were chosen, 2, 4, 12 and 20 minutes. This allowed us to study the progression of the reaction or inhibition as a function of time. This is a novel method of studying the inhibition as a function of time similar to time resolved studies.

Data (four data sets corresponding to four durations of soaking) were collected at liquid nitrogen temperature at the National Synchrotron Light Source, Brookhaven National Laboratory. Data were processed and scaled with DENZO and SCALEPACK [1]. The resolutions of the data were in the range of 1.9 to 2.35 Å.

The structures were solved by the difference Fourier method since a high resolution structure of the native intact toxin was available. The inhibitor molecules were located from Fo-Fc maps and clear density was observed.

Results

Though initially it was expected that the inhibitor molecule would bind at the active site cavity, it was found that there are two binding sites for the molecule in the intact toxin. One molecule binds in a cleft formed between the translocation domain and the catalytic domain while the other binds in a cavity close to the active site. Additionally, the latter was found to have a bound zinc ion. Presumably this inhibitor molecule first binds to the active site zinc and is transported to this cleft gradually. This is supported by the fact that the occupancy of the active site zinc decreases while the one bound to the inhibitor increases with the soaking time. However, the complete removal of zinc from the active site could not be observed. This is probably either due to the reaction being not taken to completeness or since it is a soaking experiment, BABIM did not attack every molecule in every unit cell. However, this experiment provided evidence for a novel mechanism for inhibition of the neurotoxin activity. A paper describing these results has been published [2]. (Please see Appendix 1).

(a) (b)

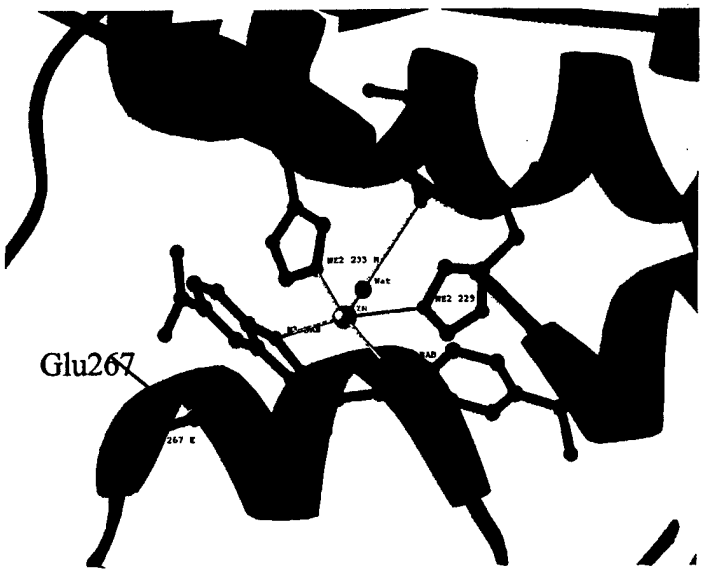

(c)

Figure 1. (a) Ribbons representation of *Clostridium botulinum* toxin B molecule with the inhibitor molecules. The inhibitor molecules and the active site residues coordinating the zinc atom are shown as ball and stick model. Zinc atoms are represented in yellow. (b) the electrostatic potential surface of the same molecule showing the cavities where the two BABIM molecules bind. (c) BABIM modeled at the active site is shown along with the RIBBONS representation of the light chain.

(2) Botulinum neurotoxin B with organic inhibitors and zinc chelators

Here a slightly different approach was followed. A few potential compounds were analyzed computationally to test whether they can be accommodated at the active site and whether energy of interaction is favorable for the molecules to bind tightly. This *virtual screening* of compounds could be done fairly rapidly before screening them by soaking the crystals.

Docking of ICD-2821 and AQF with BoNT/B

The docking studies were performed using the EUDOC program [3]. The program can be used for predicting complexes and virtual screening- identification of molecules from chemical database that can act as inhibitors. Here we have used the program for complex prediction. In essence it finds an energetically-favorable position and orientation of the ligand in the binding pocket of the receptor by a given systematic translation and rotation of the ligand in a docking box defined by the user. The

intermolecular energy of the ligand-receptor complex is used to judge the docking results and final docked models are viewed graphically with the program O [4].

We used the structure of BoNT/B refined to 1.9 Å as the receptor. The topology and coordinate files for the receptor were prepared as described by the EUDOC program. Amber 1994 force field were assigned to the receptor. In this quarter we have tried two inhibitors. 1. ICD-2821 (L-Glu-N[N-(phenoxyhydroxyphosphinyl)-L-phenylalanyl] disodium salt) is an analog of phosphoramidon and is found to be a more potent inhibitor than phosphoramidon [5]; and 2. AQF (Bz-Ala-Gln═P═(O)-Phe), a modified inhibitor of AGF (Bz-Ala-Gly═P═(O)-Phe), an inhibitor for carboxypeptidase [6]. The Gly residue was replaced by Gln to have Gln-Phe sequence which is the cleavage bond for BoNT/B.

The inhibitor molecules were built with O [4] and Antechamber, Xleap programs of Amber [7]. The ICD-2821 is a dipeptide containing Phe-Glu in which the N-terminal nitrogen of Phe is bound to a phosphorus atom and a constituent of phenyl ring attached to the phosphate oxygen. The hydrogen atoms were attached to the inhibitors and minimized by Amber. The CM2, Gteiger-Huckel charges were generated by the Antechamber program of Amber7 and assigned to the ligands. The docking results differ slightly depending on the charges assigned to them. A box of size 11 x 8 x 5 $Å^3$ was defined in the active site groove formed by the side chain of residues Asp 68, Tyr 260, Ile 263, Glu 267, Arg 369, Tye 372, Phe 373, and Ser 376. The size of the box confines the translation of center of mass of the ligand to be docked. The dimension of the box is selected so that it fits well in the active site without interfering with the side chains of the enzyme. The complex prediction was made by iterative docking of the inhibitors in the active site of BoNT/B by a systematic translation and rotation of 1 Å and 10^o respectively. The docking generates different ligand-receptor complexes by systematic combination of translation (1 Å) and rotation (10^o) within the docking box. The program lists about top 10 energetically favorable complexes based on the intermolecular interaction energy of ligand-receptor. All models are viewed graphically by O to verify the complex prediction.

The docking of ICD-2821 with BoNT/B shows that one of the phosphonyl oxygen of the inhibitor coordinates to Zn ion. The other phosphonyl O hydrogen bonds to the

backbone O of Asn 169. The Zn coordination of the phosphonyl group mimics the Zn coordination of the sulfate group of BoNT/B [8]. In this complex Zn has five coordination with four from enzyme and one from ligand. The backbone O of Glu of ICD-2821 makes hydrogen bond with OE2 of Glu 170. The phenyl ring of the modified Phe has electrostatic interactions with Tyr 372, Arg 369 and Asn 66. The phenyl ring of the benzoyl moiety of the N-terminal interacts with Glu 267 and Ala 262. The possible interactions between the ligand and enzyme are shown in Fig.2a. The intermolecular interaction energy of this complex is -34 kcal/mol.

Icd2821 Magf

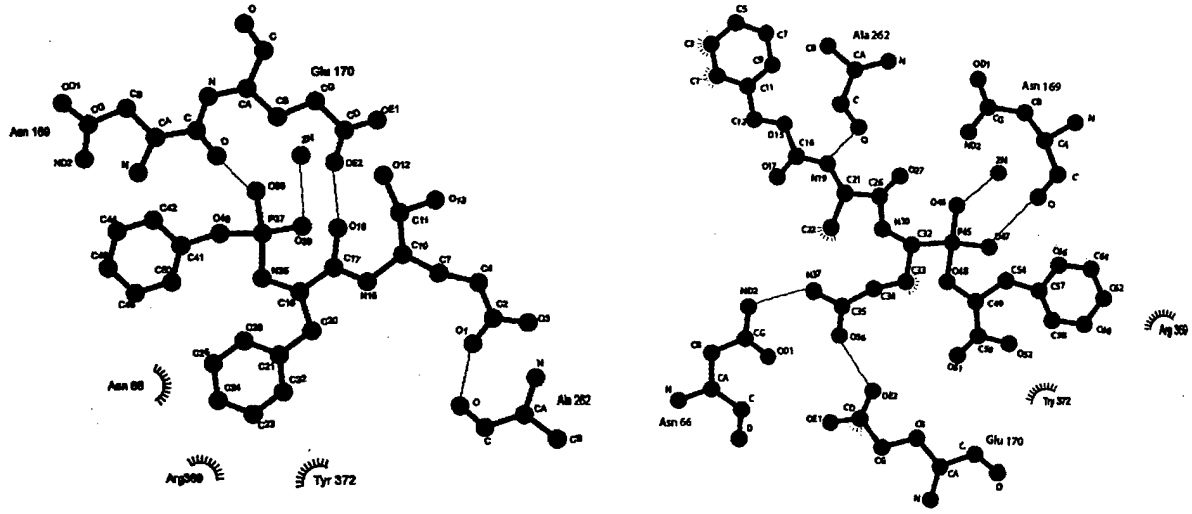

(a) (b)

Figure 2. The environment and interactions of (a) ICD-2821 and (b) MAGF with the active site residues. Zinc is shown in green. For clarity residues coordinating with zinc are not shown

The AQF is a peptide with Phe, Gln and Ala and a phosphoryl group. It is docked in a similar fashion as ICD-2821 with one of the phosphoryl oxygen coordinates to Zn and other oxygen hydrogen bonds with the backbone O of Asn 169. The side chain N and O of Gln hydrogen bonds with Asn 66 ND2 and Glu 170 OE2 respectively. The docking shows that the phenyl ring at the carboxyl group interacts with Arg 369 via π interaction. A shortest distance of 4.1Å is observed between the NE2 of Arg 369 and one

of the phenyl carbon atoms. The intermolecular interaction energy of this complex is -41 kcal/mol. The possible interactions of this model are shown in Fig. 2b.

X-ray structure of BoNT/B:ICD-2821 complex

Since we find that ICD-2821 can be reasonably fitted in the active site cavity, we proceeded with soaking experiments and co-crystallization. Crystals of BoNT/B were soaked in the mother liquor containing 1mM and 10 mM ICD-2821 overnight and 2 minutes, respectively. Crystals were flash frozen in liquid nitrogen temperature and x-ray diffraction data were collected. Though some density for the inhibitor molecule is visible, it does not account for full occupancy of the molecule. Better soaking conditions are being tried in order get full occupancy for the inhibitor molecule.

Results

Initial results are encouraging but the docking method has to be modified. In the present procedure, only the conformation of the inhibitor is allowed to change while the protein is considered to be a rigid molecule. Our initial analysis shows that this may have some limitations. An induced fit could be simulated only when both the protein and the inhibitor are allowed to change conformation. This might use lot of computer time. But for our purpose, we are interested only in finding out whether a molecule can fit into the cavity to proceed with soaking experiments. However, we realize that there may be some false negatives.

(3) Crystal structure of Clostridium botulinum B with doxorubicin

The toxicity of the neurotoxin could be inhibited at any one of the three stages of toxicity. It could be abolished by blocking the binding of toxin to the neuronal cells or by stopping the internalization of the toxin or by inhibiting the catalytic activity. In (1) and (2) the inhibition of toxicity is effected by blocking the catalytic action of the light chain. It has been shown that it is possible to block the binding site at the C-terminal fragment of the binding domain. Doxorubicin is one such molecule which binds in the same binding pocket as gangliosides. Electrospray ionization mass spectroscopy studies have shown that doxorubicin competes with gangliosides for binding. We have determined the structure of BoNT/B in complex with doxorubicin and have shown for the first time the interaction between doxorubicin and the binding domain. This work was started at the

time of the submission of the proposal and a paper was published [9]. (Please see Appendix 2).

Results

Since there are a number of doxorubicin analogs available, it may be possible to improve the binding by choosing a different analog of doxorubicin.

(4) Structural Studies with Buforin and BoNT/B

A small amount of funds were provided as a supplemental grant to collaborate with Walter Reed Army Institute of Research to study the interaction between buforin and BoNT/B via x-ray diffraction. Buforin, a 39-mer peptide, containing the scissile bond residues of BoNT/B, has been shown to inhibit the catalytic activity of the neurotoxin to some extent. Even though buforin contains the scissile bond Gln-Phe for BoNT/B, it does not cleave the bond but inhibits the catalytic activity. We determined the structure of BoNT/B crystals soaked in buforin. Interestingly, in the crystal structure, the active site zinc has been removed but we could not see and discernable density for buforin. It is clear that buforin acts on the active site to remove zinc but does not stay bound to the toxin. Co-crystallization and different soaking conditions are being tried now.

Key Research Accomplishments

- It is shown that BABIM inhibits the catalytic activity by blocking the substrate-binding site and chelating the active site zinc
- Computational screening and x-ray diffraction methods for identifying potential inhibitors work efficiently
- It is shown that doxorubicin binds in the same site as gangliosides and could be used for blocking of neurotoxins to neuronal cells
- In general, most inhibitors chelate the active site zinc and remove it from the protein making it possible for the protein to be reconstituted with zinc. It is proposed that small molecules that will not only chelate zinc but will also stay bound to the protein will be the best inhibitors

Reportable outcomes

A paper titled "A novel mechanism for *Clostridium botulinum* neurotoxin inhibition" has been published in Biochemistry in August 2002 and a reprint is enclosed as Appendix 1.

Presented an invited talk at the International meeting on Basic and Theraupeutic Aspects of Botulinum and Tetanus Toxins at Hanover, Germany in June 2002 (abstract enclosed in Appendix 3).

Presented an invited talk at the Interagency Botulinum Research Committee meeting at Madison, Wisconsin in October 2002 (abstract enclosed in Appendix 4).

Conclusions

In all our experiments we find that in the presence of putative inhibitors or chelators the active site is perturbed and the active site zinc gets disordered. When the concentration of the inhibitor is sufficient or when the duration of soaking is optimum, the zinc gets removed from the active site as seen from the absence of residual electron density for zinc in Fo-Fc maps. Also, in these cases the side chain of Glu 267, a residue coordinating with zinc loses its coordination with zinc and takes a different rotamer position. We speculate that most of the inhibitors act as chelators to remove zinc and thereby inhibit the catalytic activity. But this brings up an important issue. Since excess zinc is available in cytosol or in the body environment, it is possible for the toxin to get reconstituted with zinc and regain its activity, or the inhibition could be a "reversible" inhibition. It looks as though a search for an inhibitor which will inhibit the catalytic activity and stay bound to the toxin will be the most desirable one.

Plans for the next quarter

Crystallographic experiments with crystals soaked in other zinc chelators/inhibitors will be continued.

Personnel in the Project

1. S. Swaminathan (PI)	Scientist	20% effort
2. S. Eswaramoorthy	Asst. Scientist	50% effort
3. R. Agarwal	Research Associate	100% effort
4. D. Kumaran	Research Associate	28% effort

References

1. Otwinowski, Z. & Minor, W. (1997). Processing of X-ray diffraction data collected in oscillation mode. *Methods Enzymol.* **276**, pp. 307-326.
2. Eswaramoorthy, S., Kumaran, D. & Swaminathan, S. (2002). A novel mechanism for *Clostridium botulinum* neurotoxin inhibition. *Biochemistry* **41**, pp. 9795-9802.

3. Pang, Y.P., Perola, E., Xu, K. & Prendergast, F.G. (2001). EUDOC: A computer program for identification of drug interaction sites in macromolecules and drug leads from chemical databases. *J. Comput. Chem.* **22**, pp. 1750-1771.

4. Jones, T.A., Zou, J., Cowtan, S. & Kjeldgaard, M. (1991). Improved methods in building protein models in electron density map and the location of errors in these models. *Acta Crystallogr.* **A47**, pp. 110 - 119.

5. Adler, M., Keller, J.E., Baskin, S., Salem, H., Filbert, M.G. & Romano, J. (1999). Promising new approaches for treatment of botulinum intoxication. *J. Appl. toxicol.* **19**, pp. S5.

6. Kim, H. & Lipscomb, W.N. (1991). Comparison of structures of three carboxypeptidase A-phosphonate complex determined by x-ray crystallography. *Biochemistry* **30**, pp. 8171-8180.

7. Case, D.A., Pearlman, D.A., J.W.Caldwell, III, T.E.C., J.Wang, W.S.Ross, C.L.Simmerling, T.A.Darden, K.M.Merz, R.V.Stanton, A.L.Cheng, J.J.Vincent, M.Crowley, V.Tsui, H.Gohkl, R.J.Radmer, Y.Duan, J.Pitera, I.Massova, Seibel, G.L., U.C.Singh, P.K.Weiner & Kollman, P.A. (2002). Amber 7, University of California,: San francisco.

8. Swaminathan, S. & Eswaramoorthy, S. (2000). Structural analysis of the catalytic and binding sites of *Clostridium botulinum* neurotoxin B. *Nat. Struct. Biol.* **7**, pp. 693-699.

9. Eswaramoorthy, S., Kumaran, D. & Swaminathan, S. (2001). Crystallographic evidence for doxorubicin binding to the receptor-binding site in *Clostridium botulinum* neurotoxin B. *Acta Cryst.* **D57**, pp. 1743-1746.

A Novel Mechanism for *Clostridium botulinum* Neurotoxin Inhibition

Subramaniam Eswaramoorthy, Desigan Kumaran, and Subramanyam Swaminathan

Biology Department, Brookhaven National Laboratory, Upton, New York 11973

Biochemistry®

Reprinted from
Volume 41, Number 31, Pages 9795–9802

A Novel Mechanism for *Clostridium botulinum* Neurotoxin Inhibition†

Subramaniam Eswaramoorthy, Desigan Kumaran, and Subramanyam Swaminathan*

Biology Department, Brookhaven National Laboratory, Upton, New York 11973

Received January 18, 2002; Revised Manuscript Received May 24, 2002

ABSTRACT: *Clostridium botulinum* neurotoxins are zinc endopeptidase proteins responsible for cleaving specific peptide bonds of proteins of neuroexocytosis apparatus. The ability of drugs to interfere with toxin's catalytic activity is being evaluated with zinc chelators and metalloprotease inhibitors. It is important to develop effective pharmacological treatment for the intact holotoxin before the catalytic domain separates and enters the cytosol. We present here evidence for a novel mechanism of an inhibitor binding to the holotoxin and for the chelation of zinc from our structural studies on *Clostridium botulinum* neurotoxin type B in complex with a potential metalloprotease inhibitor, bis(5-amidino-2-benzimidazolyl)methane, and provide snapshots of the reaction as it progresses. The binding and inhibition mechanism of this inhibitor to the neurotoxin seems to be unique for intact botulinum neurotoxins. The environment of the active site rearranges in the presence of the inhibitor, and the zinc ion is gradually removed from the active site and transported to a different site in the protein, probably causing loss of catalytic activity.

Clostridium botulinum, a Gram-positive spore-forming bacterium, produces seven serotypes (A−G) of botulinum neurotoxins (BoNTs)[1] which are solely responsible for botulism causing flaccid paralysis and death (*1*, *2*). The intoxication by neurotoxins is proposed to be a four-step process (*3*−*6*): (1) cell binding, (2) internalization, (3) translocation into cytosol, and (4) enzymatic modification of a cytosolic target. The toxin first binds to the neuronal cell and then is internalized into the vesicles. To attack the targets in cytosol the neurotoxin should cross the hydrophobic barrier of the vesicle membrane. This is common to all bacterial toxins with intracellular targets and is the least understood step in the process. It is proposed that the acidification of the vesicle lumen by a proton pumping ATPase leads to conformational changes in the toxin. The acidic conformation then exposes a hydrophobic area of the toxin molecule, creates an ion channel in the membrane, and inserts the light chain (LC) into cytosol (*4*, *7*). However, not all internalized toxin molecules are translocated, the limiting factor being the reduction of the disulfide bond between heavy and light chains (*8*). Those toxin molecules not translocated are degraded in the acidic compartments. The three-dimensional structures of BoNT/A and B reveal the three structural domains corresponding to the three functions, viz., binding, translocation, and catalytic activity (*5*, *9*−*11*). The crystal structure of BoNT/B light chain with its substrate peptide fragment reveals the mode of binding of the substrate (*12*). All serotypes contain a zinc-binding motif HExxH in their catalytic domain, and their three-dimensional structures are expected to be similar in general because of significant sequence homology (*13*). However, structural details may be different, as seen between BoNT/A and BoNT/B, because of the specificity of the substrate and the scissile bond to be cleaved (*14*−*20*). The catalytic zinc is located in a deep cavity in the active site that has a wide opening for the substrate or inhibitor to enter the site. However, the deep cavity is partially covered by the belt region in BoNT/A while it is open in BoNT/B.

As of now, the treatment for botulism is a preventive one, an experimental vaccine, but no specific drug has been developed for treatment after being afflicted by botulism. Therapeutic treatments could be effective at any one of the three stages of toxicity—binding of toxin or internalization or catalytic activity (*11*). Since chelation of zinc antagonizes the neuromuscular blocking properties of botulinum neurotoxins (*21*), specific zinc chelators or inhibitors of zinc metalloproteases are being evaluated (*22*). Recently, a coumarin derivative has been tested on the light chain of botulinum neurotoxin B (*23*). Bis(5-amidino-2-benzimidazolyl)methane (BABIM), an effective zinc chelator (*24*), has been tested with BoNT/B light chain, and its IC50 (inhibition constant) is in the range of 5−10 μM (Michael Adler, personal communication). However, its effectiveness on the holotoxin is still to be studied. The crystal structure of BABIM in complex with the light chain of BoNT/B (BoNT/B-LC) has been reported (*25*). Here we present the crystal structure of a protein−inhibitor complex of intact botulinum neurotoxin type B and BABIM determined at different durations of soaking to understand the mechanism of inhibition and the probable path of entry for the inhibitor. These structures provide a series of snapshots during the reaction and reveal a possible mechanism of binding and chelation of the zinc ion.

† Research supported by the Chemical and Biological Nonproliferation Program NN20 of the U.S. Department of Energy and the U.S. Army Medical Research Acquisition Activity (Award No. DAMD17-02-2-0011) under Prime Contract No. DE-AC02-98CH10886 with Brookhaven National Laboratory. D.K. was partly supported by funds from Veterans Administration Medical Center, Pittsburgh.

* To whom correspondence should be addressed. Telephone: (631) 344-3187. Fax: (631) 344-3407. E-mail: swami@bnl.gov.

[1] Abbreviations: BoNT, botulinum neurotoxin; LC, light chain; BABIM, bis(5-amidino-2-benzimidazolyl) methane; NSLS, the National Synchrotron Light Source.

10.1021/bi020060c CCC: $22.00
Published on Web 07/13/2002

Table 1: Crystal Data and Refinement Statistics

cell parameters: $a = 75.92$, $b = 123.24$, $c = 95.90$ Å, and $\beta = 113.7$ °. space group $P2_1$				
PDB idcode	1G9B	1G9D	1G9A	1G9C
		Data Collection		
soaking time (min)	2	4	12	20
resolution (Å)	50.0−1.9	50.0−2.2	50.0−2.0	50.0−2.35
total number of reflections	297 330	295 435	308 578	224 958
number of unique reflections	104 669	81 518	95 973	64 852
completeness[a] (%)	82.7 (18.4)	97.4 (92.0)	84.5 (16.1)	98.6 (91.0)
R_{merge}[b] (R_{merge} last shell)	0.062 (0.45)	0.064 (0.38)	0.063 (0.46)	0.058 (0.35)
$\langle I/\sigma(I)\rangle$	12.5	12.6	9.7	10.6
		Refinement		
resolution (Å)	50.0−2.0	50.0−2.2	50.0−2.1	50.0−2.35
number of reflections (overall completeness)	93 756 (86.3)	69 919 (90.7)	83 496 (88.8)	60 645 (93.1)
$F/\sigma(F)$ cutoff value	0	0	0	0
R_{free}[c]	0.243	0.283	0.248	0.247
R_{work}[c]	0.213	0.263	0.213	0.210
RMSD				
bond lengths (Å)	0.007	0.007	0.007	0.007
bond angles (deg)	1.37	1.44	1.38	1.40
number of atoms				
protein	10 587	10 587	10 587	10 587
water molecules	548	383	546	422
inhibitor	50	50	50	50
Zn (partially occupied)	2	2	2	2
occupancy of Zn1 (B Å^2)	0.65(51.1)	0.59(61.5)	0.56(59.3)	0.50(54.1)
occupancy of Zn2 (B Å^2)	0.35(50.3)	0.41(71.1)	0.44(59.8)	0.50(56.4)
$\langle B\rangle$ protein (Å^2)	29.6	30.6	31.0	31.9

[a] Completeness for the highest bin is given within parentheses. Outermost shell: 2.02−1.9 (1G9B), 2.28−2.20 (1G9D), 2.13−2.0 (1G9A), and 2.43−2.35 (1G9C). [b] $R_{merge} = \Sigma_j(|I_h - \langle I\rangle_h|)/\Sigma I_h$, where $\langle I_h\rangle$ is the average intensity over symmetry equivalents. [c] $R = \Sigma|F_{obs} - F_{calc}|/\Sigma|F_{obs}|$; R_{work} is summed over reflections used in refinement, and R_{free} is summed over reflections set aside for validation.

MATERIALS AND METHODS

Preparation of Protein for Crystallization. Intact neurotoxin was purchased from the Food Research Institute (Madison, WI). Since the BoNT endopeptidase activity is expressed only after the disulfide bond is reduced (*26*), preparation of protein for crystallization was slightly modified from the published procedure (*27*). Also, because the protein is supplied as a precipitate in ammonium sulfate, a sulfate ion was found to be present in the catalytic site (*10*). Since the sulfate ion might possibly hinder inhibitor binding, the sulfate ion was removed before crystallization. The protein was dialyzed against 100 mM NaCl, 50 mM Hepes, and 10 mM dithiothreitol at pH 7.0 overnight in two steps. Then 80 mM barium acetate was added to the dialysate to remove the sulfate ion bound in the catalytic site and dialyzed twice again. The final dialysis was done without barium acetate. Crystallization condition is as described but under reducing condition (*27*).

Inhibitor Soaking. Initially, various concentrations of BABIM and durations of soaking were tried to test the stability of the crystal and its diffraction quality. The optimum concentration of BABIM for soaking was determined as 3 mM, since at higher concentrations the crystals dissolved within a short duration of soaking or the crystal quality became extremely poor and at lower concentrations BABIM could not be seen in the electron density maps. Because the goal was to study the inhibition mechanism, crystals were soaked for different duration. Crystals were soaked for 2, 4, 12, and 20 min in the cryoprotectant solution containing BABIM and immediately frozen to liquid nitrogen temperature, by plunging the crystal into a vial of liquid nitrogen, to stop the reaction. For soaking durations larger than 20 min, either the crystals dissolved or the diffraction was extremely poor. Neither varying the molecular weight of the precipitant (PEG) nor increasing the precipitant concentration helped.

Data Collection. Data were collected at liquid nitrogen temperature at the x12C beamline of the NSLS, Brookhaven National Laboratory with Brandeis CCD based B1 detector. An oscillation range of 1° was used for each data frame, and data corresponding to 200° in ϕ were collected with crystal to detector distance of 100 mm and $\lambda = 1.01$ Å. Data were reduced with DENZO and SCALEPACK (*28*). Data collection statistics are presented in Table 1. In the case of two data sets, a resolution cutoff has been used in the refinement since the completion in the highest resolution shell was less than 20% and R_{merge} was high.

Structure Determination. Initial model coordinates were obtained from PDB idcode 1epw. After initial rigid body refinement, the structures were refined with CNS (*29*). Adjustments of the original model was done with 'O' (*30*). The protein model is complete except for residues 440, 441, and 442, which are in the proteolytic site. A σA-weighted Fo−Fc map was calculated with refined models, and clear continuous residual density could be seen for the inhibitor molecules (Figure 1a,b). The starting model for BABIM was taken from Katz et al. (*24*). The model was further refined with the inhibitor and water molecules included. Refinement statistics are included in Table 1. Structures were validated with PROCHECK (*31*).

RESULTS AND DISCUSSION

Description of the Structure. Two inhibitor molecules are bound to the holotoxin and give a clue to probable pathways

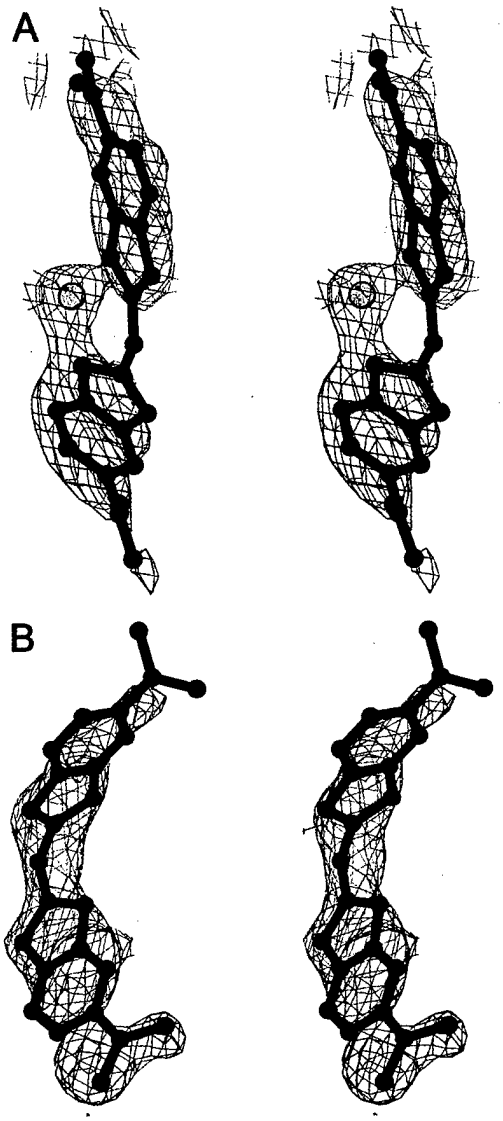

FIGURE 1: Stereoview of 2Fo−Fc maps. σA-weighted 2Fo−Fc maps superposed on the refined positions of BABIM1 (a) and BABIM2 (b). Contours are drawn at 1σ. Zinc atom bound to BABIM is shown in yellow. The density is weak for C9 of BABIM1 and for N1 and N2 of BABIM2.

for them to enter the active site (Figure 2a−c). A cleft formed between the translocation domain and the catalytic domain is connected to the active site cavity (cavity 1), and both of them form part of a tunnel (Figure 2b,c). This tunnel is lined by negatively charged atoms and accordingly has a negative electrostatic potential. Asp 375 of the catalytic domain lies midway in this tunnel and is hydrogen bonded to Thr 713 through a water molecule and acts like a gate (Figure 3a,b). Interestingly, this network of hydrogen bonds separates the two BABIM molecules, suggesting that there are two pathways for the inhibitor to enter the molecule (Figure 2b,c). It is proposed that one inhibitor molecule (BABIM2) has entered through this cleft between the translocation and catalytic domains. Since Asp 375 prevents it from moving through the channel any further, it stays there because of favorable interactions.

Inhibitor Binding Sites. Inhibitor molecule BABIM2 sits in the cleft formed between the translocation and binding domains and makes contacts with both the catalytic and translocation domains. The inhibitor is near residue Lys 720 and Asp 375 (Figure 3c). The side chains of residues Asp 375 and Lys 720 interact with the π-electron clouds of one of the benzimidazolyl groups. Nζ of Lys 720 also makes hydrogen bond with N4′ of BABIM2. N1 and N2 of the inhibitor make hydrogen bonds with NH2 of Arg 217 and Nδ2 of Asn 203. N3 and N4′ make hydrogen bonds with Oδ1 of Asp 452. N3′ of the benzimidazolyl group makes hydrogen bond with O of Asp 452. N2′ interacts with O of Asp 447 through a water molecule besides hydrogen bonding to O of Phe 537. N1′ interacts with the OH of Tyr 724. The hydrogen-bonding contacts are listed in Table 2.

When the catalytic domain (L chain) is considered in isolation along with the belt region, one more cavity (cavity 2) in addition to the deep and wide open active site cavity (cavity 1) could be identified (Figure 2c). Residues 373−375 and 454−457 are along the opening of this cavity. At the bottom, this cavity opens up into the active site cavity, and hence there is a continuous channel from the active site cavity up to the top of cavity 2. However, when the holotoxin is considered as a whole, part of one of the long α helices (residues 709−713) is up against this opening, transforming it into a small pocket. This pocket becomes part of the tunnel. The inhibitor molecule, BABIM1, enters this pocket, presumably through the wide opening of the active site cavity and stays bound to the protein (Figure 3a,b). One of the amidino groups interacts with the active site residues, while the other amidino group nitrogens make many contacts with the translocation domain. One of the amidino groups of BABIM1 is between Arg 369 and Tyr 372. N1 of the amidino group hydrogen bonds to NH1 of Arg 369. The benzimidazole nitrogen atoms N3 and N4 are making hydrogen bonds with catalytic domain. N3 makes hydrogen bond to Oδ1 of Asp 68, and N4 makes hydrogen bonds with O of Ser 374 and Oγ of Ser 376. N4′ of BABIM1 interacts with Oε1, O, and Oδ1 of Gln 258, Glu 451, and Asp 375, respectively. N1′ and N2′ of the other amidino group interact with the translocation domain. N1′ is hydrogen bonded to Oγ1 of Thr 713. N2′ is hydrogen bonded to O and Oγ1 of Thr 709 and O of Phe 455.

Perturbation of the Active Site. The active site has been mapped in the structure of holotoxin BoNT/B determined to 1.7 Å resolution (S. Eswaramoorthy and S. Swaminathan, unpublished data). The zinc ion in the active site is coordinated to residues His 229, His 233, Glu 267, and a water molecule. The inhibitor molecules in the present structure do not stay bound to Zn through coordination, as observed in serine proteases and in BoNT/B-LC:BABIM complex (*24*, *25*). However, the active site environment in the present structure is perturbed, probably due to the presence of BABIM (Figure 4). Significantly, the coordination between the Zn and Glu 267 is lost, and the side chain of Glu 267 takes a different rotamer position to make a hydrogen bond to Gln 264 (Table 2). The inhibitor might be competing with Glu 267 for a possible coordination to Zn. A composite-omit map shows a water molecule in the place of Oε1 of Glu 267 coordinating to Zn besides the presumed nucleophilic water. This water molecule is hydrogen bonded to Zn and the carbonyl oxygen of Glu 267. The nucleophilic water molecule coordinating with Zn is making a hydrogen bond to Oε2 of Glu 230. The water molecules are 2.4 and 2.6 Å away from the Zn; also, one of the histidine

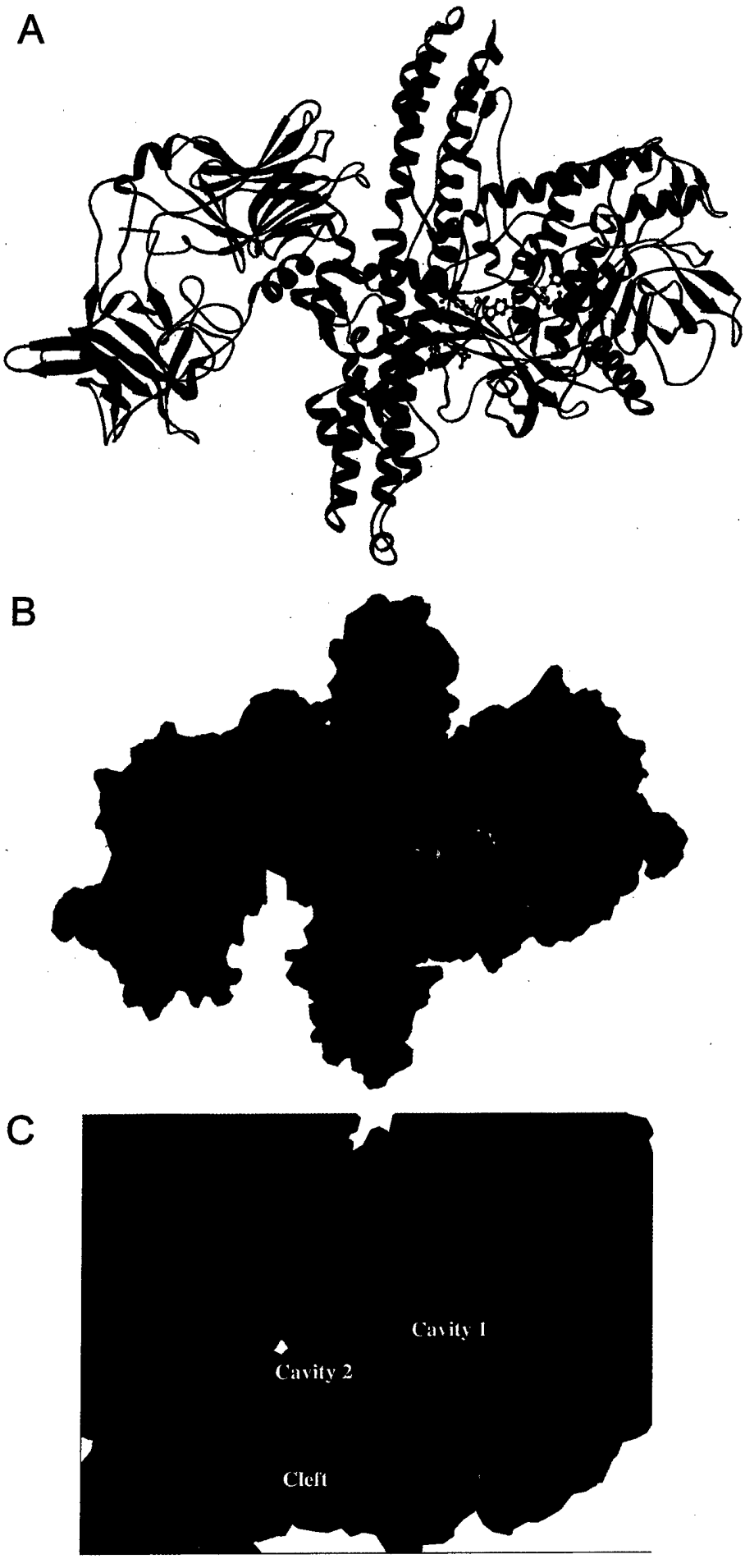
A
B
C
Cavity 1
Cavity 2
Cleft

coordination distances has become longer (2.6 Å). The coordination of the Zn and the above-mentioned residues were very strong in the holotoxin, unlike in this structure. This somewhat larger coordination distances and loss of coordination with Glu 267 make Zn binding less stable. Since Zn plays a structural role also and its removal changes the tertiary structure, the protein itself may become unstable (*32*, *33*). This may be an intermediate stage before the Zn gets removed completely and the structure collapses. This is supported by the fact that the crystal dissolves when BABIM concentration in the mother liquor is increased or if the crystal is soaked for a longer duration.

Novel Binding and Inhibition Mechanism. The catalytic domain has a wide and deep cavity at the active site. The cleavage and binding sites in the substrate are different and separated, and the binding region is essential for the cleavage of scissile bond. Though the substrate synaptobrevin is a large molecule, biochemical studies have shown that a minimum length of 51 peptides containing the binding and the cleavage regions is enough for cleavage of the substrate to take place (*34*). The substrate partly takes the position of the belt region in the crystal structure of the light chain:synaptobrevin complex and extends on both sides of the active site with the region around the scissile bond to be cleaved protruding inside the opening and approaching close to the zinc site (*12*). The substrate binds to the protein between the loops 50 and 250 where the light chain would be interacting with the translocation domain in the holotoxin. In the structures reported here, BABIM1 and 2 partially occupy the synaptobrevin site and would block the binding of the substrate to the toxin eventually blocking the cleavage activity. The binding of two inhibitor molecules to the toxin molecule reveals an unexpected binding mechanism of the inhibitor.

Residues Arg 369 and Tyr 372 are presumably involved in the protease activity (*26*). In the structure of the BoNT/B-LC:synaptobrevin complex, the cleaved residues of the substrate, synaptobrevin-II, are supposedly stabilized by the protein residues Arg 369 and Tyr 372, which suggests that spatially they must have been close to the scissile bond to be cleaved. In this structure the BABIM1 binding mimics this intermediate state of substrate binding. The amidino group lies between Arg 369 and Tyr 372 with N1 of the inhibitor hydrogen bonded to Arg 369. The catalytic activity might be blocked either by the nonavailability of this donor atom or because the substrate binding is blocked.

We propose a mechanism for zinc chelation as seen in this study. To do a time-dependent study of inhibitor binding, we soaked crystals in mother liquor containing 3 mM of the inhibitor for various periods of time, and the reaction was presumably stopped by immediately freezing the crystals to liquid nitrogen temperature. Experiments done with approximate soaking times of 2, 4, 12, and 20 min are reported in this study. Because of the disruption of the coordination, the temperature factor of the zinc ion increased with the soaking time. Simulated omit maps brought out two peaks which could be modeled as partially occupied zinc atoms—one in the original site and the other bound to BABIM1 by chelating nitrogens N3 and N3′ and to Nϵ2 of Gln 258. The combined peak heights of the partially occupied zinc atoms were comparable to that of a fully occupied zinc atom in structures of the same protein at similar resolution. Assuming that there is one zinc atom per molecule, occupancies were assigned on the basis of the relative peak heights in the difference Fourier maps. For BABIM1, occupancies were set equal to that of the bound zinc. Interestingly, as the soaking time increases, the occupancy of the original zinc

Table 2: Hydrogen Bonding and Other Interactions Involving BABIM1, BABIM2, and Zn[a]

residue	atom name	residue and atom name	distance (Å)
		BABIM1	
BAB	N1	NH1 R369	3.18
BAB	N3	OD1 D68	3.24
BAB	N4	O S374	2.63
BAB	N4	OG S376	3.40
BAB	N4′	OE1 Q258	2.54
BAB	N4′	O E451	2.64
BAB	N4′	OD1 D375	3.00
BAB	N2′	O F455	2.40
BAB	N2′	O T709	3.14
BAB	N2′	OG1 T709	2.93
BAB	N1′	OG1 T713	2.40
BAB	N3	Zn2	2.41
BAB	N3′	Zn2	2.50
Zn2		NE2 Q258	2.55
		BABIM2	
BAB	N1	NH2 R217	2.60
BAB	N2	ND2 N203	2.58
BAB	N3	OD1 D452	2.52
BAB	N4′	OD1 D452	3.18
BAB	N4′	NZ K720	3.18
BAB	N3′	O D452	2.82
BAB	N2′	O F537	2.99
BAB	N2′	O water	2.60
BAB	N1′	OH Y724	2.89
		Perturbed Active Site	
zinc	Zn	NE2 H229	2.32
zinc	Zn	NE2 H233	2.15
zinc	Zn	O water	2.40
zinc	Zn	O water	2.42
water	O	OE2 E230	3.26
water	O	O E267	2.96
E267	OE2	N Q264	2.64

[a] The high and low cutoff values used for hydrogen bond distances and angles are 3.5 Å and 120°, respectively.

FIGURE 2: (a) RIBBONS (*35*) representation of BoNT/B. Helices in blue represent 3_{10} helices. Two molecules of BABIM and the zinc site residues are shown as ball-and-stick model. The two partially occupied zinc atoms are shown in yellow, while water molecules are in silver gray. (b) Grasp (*36*) representation of the electrostatic potential surface of BoNT/B. BABIM1 and 2 trapped in the tunnel and the residues coordinating zinc are shown as sphere model. Zn atoms are shown in yellow, while water molecules coordinating with active site Zn are in silver gray. Glu 267 moves away from Zn with one of the water molecules replacing its coordination. The top of the tunnel wall is clipped for clarity by excluding residues 67−68, 253−261, 431−455, and 525−532 from the model. Asp 375 (shown in black) lies between BABIM1 and 2 (labeled as 1 and 2). The positive and negative electrostatic potentials are represented in blue and red. (c) An enlarged view of the BABIM1 and 2 binding site. BABIM1 and 2 and the active site residues shown in panel b are not included in this figure for clarity. Cavity 1 is the wide and deep active site cavity. Cavity 2 would have an opening in the isolated light chain but in intact toxin is blocked by the long helices of the translocation domain as shown here and connects cavity 1 and the cleft between the translocation and catalytic domain to form a channel.

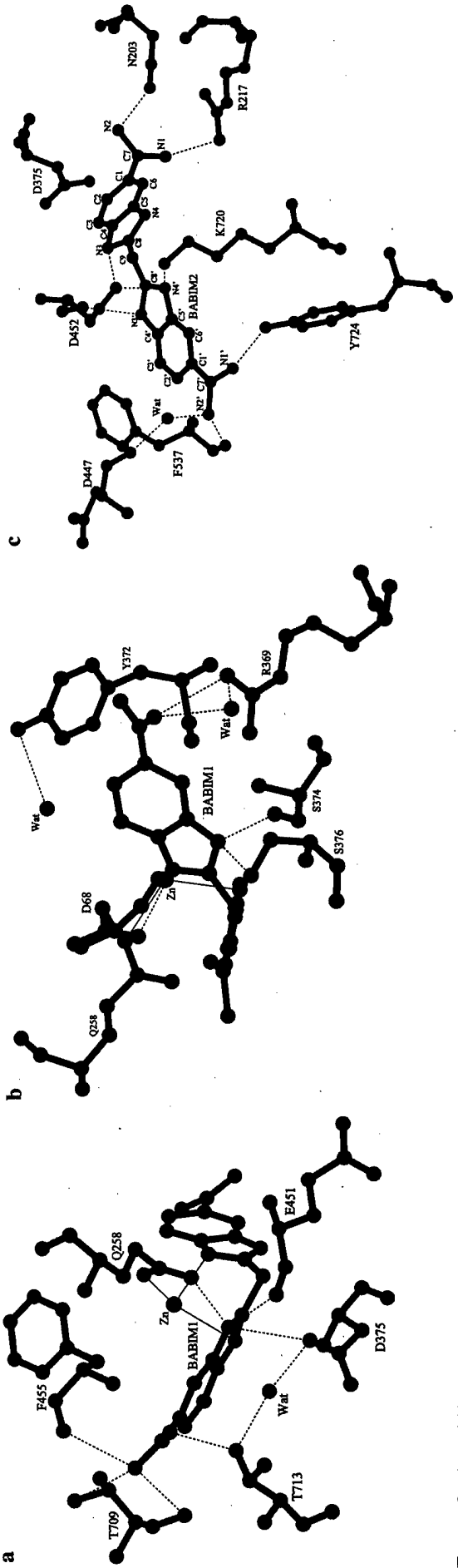

FIGURE 3: (a and b) Residues interacting with BABIM1. For clarity, residues surrounding each amidinobenzimidazolyl groups are given separately. Hydrogen bonds are shown as dashed line, while the metal coordinations are as thin solid lines. As shown here and in Table 2, BABIM1 interacts with both the translocation and catalytic domains. (c) Residues interacting with BABIM2. Hydrogen bond interactions are listed in Table 2 and shown here in dashed lines. Asp 375 and Lys 720 lie on either side of one of the benzimidazolyl group and their interactions are mostly π-interactions.

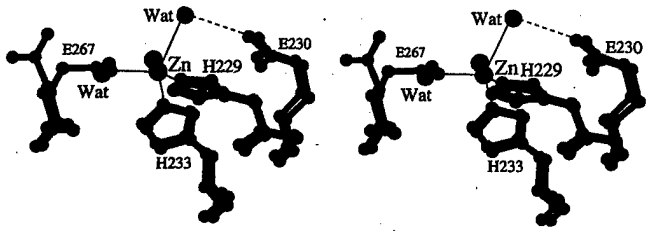

FIGURE 4: Stereoview of the superposition of the unperturbed (in green) and the perturbed states (red) of the active site. The active site residues are perturbed when crystals are complexed with BABIM. The side chain of Glu 267 takes a different orientation, and a water molecule replaces the carboxylate group. Coordinating distance between Zn and Nϵ2 of His 229 has increased to more than 2.6 Å. Figures 1, 3, and 4 were produced with MOLSCRIPT (*37*).

ion decreases, while the one bound to BABIM1 increases (Table 1). When the crystal was soaked for 1 min or less, though BABIM could not be located in the difference map, the perturbation of zinc coordination was evident (data not shown). We believe that BABIM1 binds to the zinc ion and moves it away from the active site to a position where interactions for it to bind to the protein are more favorable. Since the soaking was done for a very short duration and the crystal was flash frozen, it is possible that the reaction was not taken to completion and what we see is an average structure of a transitory state. Partial occupancy and high thermal factors for zinc ions indicate that the zinc ion has not been completely removed from the protein. Probably the reaction was halted before BABIM could attack every molecule in every unit cell of the crystal. The mode of zinc binding to BABIM1 suggests that initially BABIM1 should have bound to the active site zinc via N3 and N3′ of BABIM. However, since the experiment was done by soaking crystals in the mother liquor containing BABIM, it was not possible to see the instantaneous binding of BABIM1 to the active site zinc. Extrapolating from the conformation of BABIM1 and the bound zinc, we modeled this binding mode (Figure 5). Since Glu 267 had already taken a different rotamer position and other side chains in this region were perturbed, we could model this without disturbing the protein model. The model was built with 'O' (*30*) and energy minimized with CNS, and it seems to be energetically favorable since the cavity is wide open. An ideal experiment would be to soak the crystal for an optimum duration for the reaction to be completed. However, this was not possible, since crystals dissolve if soaked longer in BABIM solution, suggesting that the crystal becomes unstable when zinc is removed.

In the present study, we find two BABIM molecules bound to the protein, while in the crystal structure of BoNT/B-LC with BABIM, there is only one bound BABIM since it lacks the heavy chain altogether. Also in the present study, the zinc is coordinated with N3 and N3′ of BABIM1, and the torsion angle C8−C9−C8′−N3′ is 147°, an energetically favorable conformation. In the crystal structure of BoNT/B-LC:BABIM, the zinc is coordinated with N1′ and N2′ of BABIM, and the inhibitor molecule is planar, with C8−C9−C8′−N3′ equal to 179°.

CONCLUSION

The advent of cryocrystallography has now made it possible to study the enzymatic reactions via X-ray crystal-

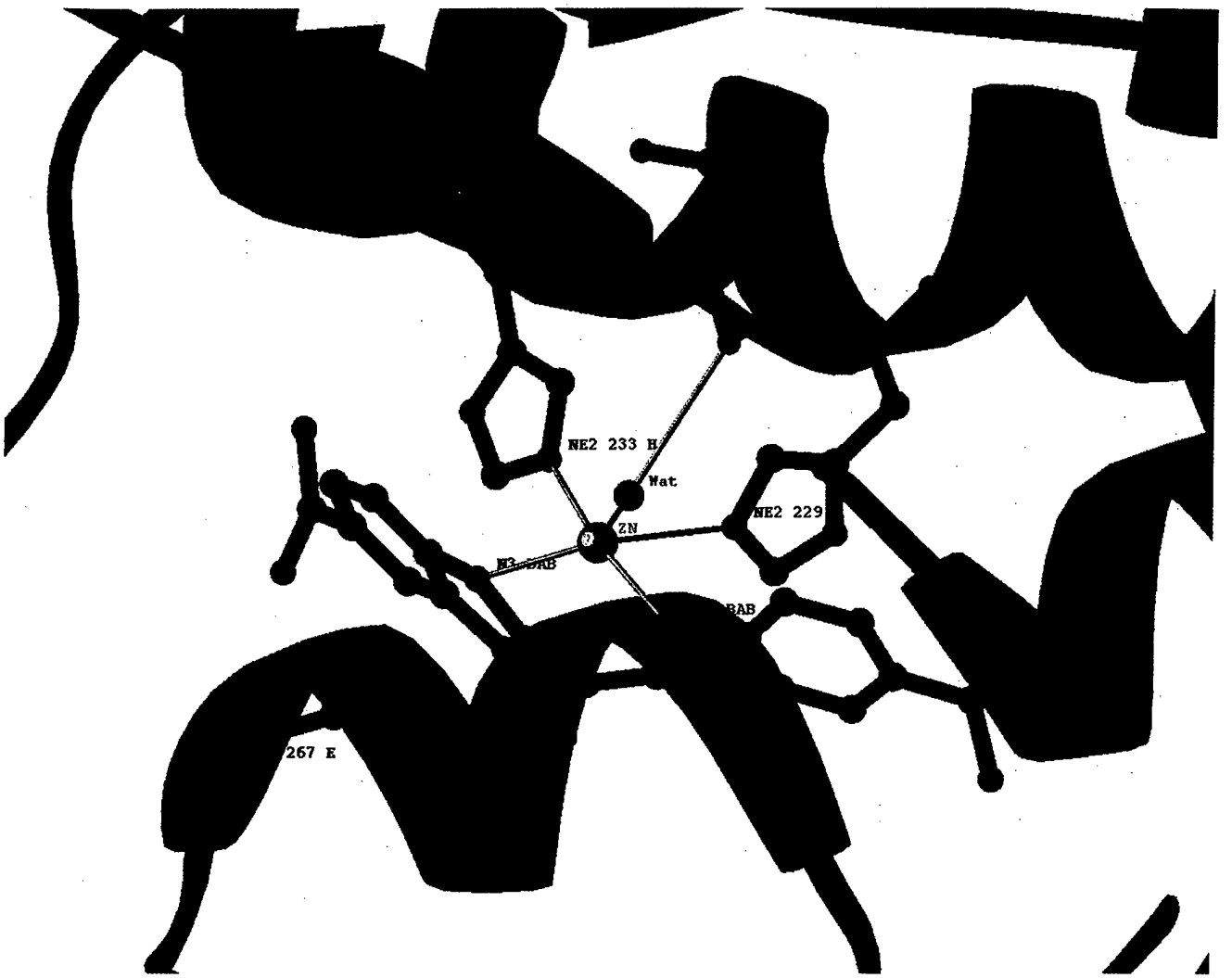

FIGURE 5: BABIM modeled at the active site is shown along with RIBBONS (*35*) representation of the light chain and the belt region. The mode of binding of zinc was assumed to be similar to that of BABIM1. There was no disruption to the active site, since the perturbation of the side chains is already taken into consideration and the side chain of Glu 267 has already moved away from zinc. This model is similar to Katz et al. (*24*). Coordination to zinc ion from protein ligands and the inhibitor are shown as thin yellow lines.

Table 3: Data Statistics for Each Data Set[a]

				1G9B						
resol. bins (Å)	50.0-4.35	3.45	3.02	2.74	2.54	2.39	2.27	2.17	2.09	2.0
completeness	99.0	99.5	99.5	99.0	97.5	96.5	94.6	89.1	80.9	65.1
R_{merge}	0.031	0.036	0.052	0.082	0.126	0.167	0.211	0.247	0.292	0.324
				1G9D						
resol. bins (Å)	50.0-4.74	3.76	3.29	2.99	2.77	2.61	2.48	2.37	2.28	2.20
completeness	98.8	99.7	99.5	99.2	98.9	98.1	96.6	96.9	96.0	92.7
R_{merge}	0.033	0.040	0.055	0.103	0.131	0.164	0.246	0.312	0.319	0.375
				1G9A						
resol. bins (Å)	50.0-4.58	3.63	3.17	2.88	2.68	2.52	2.39	2.29	2.20	2.10
completeness	99.4	100.0	100.0	100.0	100.0	100.0	99.5	95.2	85.3	70.6
R_{merge}	0.043	0.055	0.073	0.102	0.149	0.204	0.259	0.300	0.349	0.380
				1G9C						
resol. bins (Å)	50.0-5.06	4.02	3.51	3.19	2.96	2.79	2.65	2.53	2.43	2.35
completeness	100.0	100.0	100.0	100.0	99.9	99.6	99.5	99.0	96.7	91.0
R_{merge}	0.036	0.042	0.055	0.078	0.109	0.160	0.216	0.276	0.332	0.352

[a] For 1G9B and 1G9A, the completeness and the R_{merge} for the resolution bin not used in the refinement are given in Table 1.

lography, though with some limitations, and we have used this technique to study the inhibition mechanism as a function of time. In summary, the structure of BoNT/B in complex with an inhibitor, BABIM, shows that the active site residues rearrange in the presence of the inhibitor and the active site zinc is progressively removed. The inhibitor partly occupies the site where the substrate would bind and blocks it from binding to the toxin. We have also shown that it is possible for appropriate inhibitors to enter the active site of the holotoxin. However, the inhibition could be due to either the nonavailability of substrate-binding sites or the removal of zinc or a combination of both.

APPENDIX

Coordinates. Atomic coordinates have been deposited in the Protein Data Bank. Accession codes are 1G9A, 1G9B, 1G9C, and 1G9D, as given in Table 3.

ACKNOWLEDGMENT

We thank Drs. D. H. Rich and T. Oast, University of Wisconsin, for the generous gift of BABIM and Drs. M. Adler and B. R. Singh for useful discussions. We thank the reviewers for their helpful comments.

REFERENCES

1. Sathyamurthy, V., and Dasgupta, B. R. (1985) *J. Biol. Chem. 260*, 10461−10466.
2. Schiavo, G., Matteoli, M., and Montecucco, C. (2000) *Physiol. Rev. 80*, 717−766.
3. Schantz, E. J., and Johnson, E. A. (1992) *Microbiol. Rev. 56*, 80−99.
4. Menestrina, G., Schiavo, G., and Montecucco, C. (1994) *Mol. Aspects Med. 15*, 79−193.
5. Montecucco, C., and Schiavo, G. (1994) *Mol. Microbiol. 13*, 1−9.
6. Oguma, K., Fujinaga, Y., and Inoue, K. (1995) *Microbiol. Immunol. 39*, 161−168.
7. Schiavo, G., Rossetto, O., and Montecucco, C. (1994) *Semin. Cell Biol. 5*, 221−229.
8. de-Paiva, A., Poulain, B., Lawrence, G. W., Shone, C. C., Tauc, L., and Dolly, J. O. (1993) *J. Biol. Chem. 268*, 20838−20844.
9. Lacy, D. B., Tepp, W., Cohen, A. C., DasGupta, B. R., and Stevens, R. C. (1998) *Nat. Struct. Biol. 5*, 898−902.
10. Swaminathan, S., and Eswaramoorthy, S. (2000) *Nat. Struct. Biol. 7*, 693−699.
11. Montecucco, C., Papini, E., and Schiavo, G. (1994) *FEBS Lett. 346*, 92−98.
12. Hanson, M. A., and Stevens, R. C. (2000) *Nat. Struct. Biol. 7*, 687−692.
13. Schiavo, G., Rossetto, O., Santucci, A., Dasgupta, B. R., and Montecucco, C. (1992) *J. Biol. Chem. 267*, 23479−27483.
14. Schiavo, G., Shone, C. C., Rossetto, O., Alexander, F. C. G., and Montecucco, C. (1993) *J. Biol. Chem. 268*, 11516−11519.
15. Schiavo, G., Benfenati, F., Poulain, B., Rossetto, O., de-Lauretto, P. P., Dasgupta, B. R., and Montecucco, C. (1992) *Nature 359*, 832−835.
16. Blasi, J., Chapman, E. R., Yamasaki, S., Binz, T., Niemann, H., and Jahn, R. (1993) *EMBO J. 12*, 4821−4828.
17. Schiavo, G., Santucci, A., Dasgupta, B. R., Metha, P. P., Jontes, J., Benfenati, F., Wilson, M. C., and Montecucco, C. (1993) *FEBS Lett. 335*, 99−103.
18. Schiavo, G., Rossetto, O., Catsicas, S., Polverino-de-Laureto, P., Dasgupta, B. R., Benfenati, F., and Montecucco, C. (1993) *J. Biol. Chem. 268*, 23784−23787.
19. Schiavo, G., Malizio, C., Trimble, W. S., Polverino-de-Laureto, P., Milan, G., Sugiyama, H., Johnson, E. A., and Montecucco, C. (1994) *J. Biol. Chem. 269*, 20213−20216.
20. Söllner, T., Whiteheart, S. W., Brunner, M., Erdjument-Bromage, H., Geromanos, S., Tempst, P., and Rothman, J. E. (1993) *Nature 362*, 318−324.
21. Simpson, L. L., Coffield, J. A., and Bakry, N. (1993) *J. Pharmacol. Exp. Ther. 267*, 720−727.
22. Auld, D. S. (1995) *Methods Enzymol. 248*, 228−242.
23. Adler, M., Nicholson, J. D., and Hackley, B. E. (1998) *FEBS Lett. 429*, 234−238.
24. Katz, B. A., Clark, J. M., Finer-Moore, J. S., Jenkins, T. E., Johnson, C. R., Ross, M. J., Luong, C., Moore, W. R., and Stroud, R. M. (1998) *Nature 391*, 608−612.
25. Hanson, M. A., Oost, T. K., Sukonpan, C., Rich, D. H., and Stevens, R. C. (2000) *J. Am. Chem. Soc. 122*, 11268−11269.
26. Li, L., Binze, T., Niemann, H., and Singh, B. R. (2000) *Biochemistry 39*, 2399−2405.
27. Swaminathan, S., and Eswaramoorthy, S. (2000) *Acta Crystallogr., Sect. D 56*, 1024−1026.
28. Otwinowski, Z., and Minor, W. (1997) *Methods Enzymol. 276*, 307−326.
29. Brunger, A. T., Adams, P. D., Clore, G. M., Delano, W. L., Gros, P., Grosse-Kunstleve, R. W., Jiang, J. S., Kuszwewski, J., Nilges, M., Pannu, N. S., Read, R. J., Rice, L. M., Somonsom, T., and Warren, G. L. (1998) *Acta Crystallogr., Sect. D 54*, 905−921.
30. Jones, T. A., Zou, J., Cowtan, S., and Kjeldgaard, M. (1991) *Acta Crystallogr., Sect. A 47*, 110−119.
31. Laskowski, R. A., MacArthur, M. W., Moss, D. S., and Thornton, J. M. (1993) *J. Appl. Crystallogr. 26*, 283−291.
32. Fu, F., Lomneth, R. B., Cai, S., and Singh, B. R. (1998) *Biochemistry 37*, 5267−5278.
33. Li, L., and Singh, B. R. (2000) *Biochemistry 39*, 10581−10586.
34. Foran, P., Shone, C. C., and Dolly, J. O. (1994) *Biochemistry 33*, 15365−15374.
35. Carson, M. (1991) *J. Appl. Crystallogr. 24*, 958−961.
36. Nicholls, A., Sharp, K., and Honig, B. (1991) *Proteins 11*, 281−296.
37. Kraulis, P. J. (1991) *J. Appl. Crystallogr. 24*, 946−950.

BI020060C

Acta Crystallographica Section D
Biological Crystallography
ISSN 0907-4449

Crystallographic evidence for doxorubicin binding to the receptor-binding site in *Clostridium botulinum* neurotoxin B

S. Eswaramoorthy, D. Kumaran and S. Swaminathan*

Biology Department, Brookhaven National Laboratory, Upton, NY 11973, USA

Correspondence e-mail: swami@bnl.gov

Received 25 June 2001
Accepted 13 August 2001

PDB Reference: BoNT/B–doxorubicin complex, 1i1e.

The neurotoxins of *Clostridium botulinum* and tetanus bind to gangliosides as a first step of their toxin activity. Identifying suitable receptors that compete with gangliosides could prevent toxin binding to the neuronal cells. A possible ganglioside-binding site of the botulinum neurotoxin B (BoNT/B) has already been proposed and evidence is now presented for a drug binding to botulinum neurotoxin B from structural studies. Doxorubicin, a well known DNA intercalator, binds to the neurotoxin at the receptor-binding site proposed earlier. The structure of the BoNT/B–doxorubicin complex reveals that doxorubicin has interactions with the neurotoxin similar to those of sialyllactose. The aglycone moiety of the doxorubicin stacks with tryptophan 1261 and interacts with histidine 1240 of the binding domain. Here, the possibility is presented of designing a potential antagonist for these neurotoxins from crystallographic analysis of the neurotoxin–doxorubicin complex, which will be an excellent lead compound.

1. Introduction

C. botulinum and tetanus neurotoxins belong to the same class of neurotoxins and share significant sequence homology. They possess similar structural and functional domains and have a similar mechanism of toxicity (Simpson, 1986). However, botulinum neurotoxins act at the neuromuscular junction (NMJ) causing flaccid paralysis, while tetanus toxin acts at the central nervous system (CNS) causing spastic paralysis (Schiavo *et al.*, 2000). These neurotoxins are potential biowarfare agents and are also a significant public health problem. There are no known antidotes available either for tetanus or for botulinum neurotoxins.

C. botulinum toxins follow a four-step mechanism (Montecucco *et al.*, 1994); they bind to the neuronal cells, are internalized into the vesicles and translocated into the cytosol, where they attack specific components of SNARE proteins to cleave them at specific peptide bonds causing inhibition of formation of SNARE complex and thereby blocking neurotransmitter release (Söllner *et al.*, 1993). Clostridium neurotoxins comprise two chains, an N-terminal light chain of 50 kDa (LC) and a C-terminal heavy chain of 100 kDa (HC), held together by a single disulfide bond. The heavy chain is responsible for binding, internalization and translocation, while the light chain is responsible for catalytic activity inside the cytosol. Neurotoxins bind to the neuronal cells *via* gangliosides and negatively charged lipids on the surface of the cell (Menestrina *et al.*, 1994). A double-receptor model, with low-affinity binding to gangliosides and high-affinity binding to a protein receptor, has been proposed and a protein receptor has been identified (Montecucco, 1986). The catalytic domain is a zinc endopeptidase containing an HE*xx*H zinc-binding motif (Schiavo *et al.*, 1994).

Antagonists for these neurotoxins could act in three ways (Adler *et al.*, 1998). They could either be molecules which attach to the binding site, thereby inhibiting binding of neurotoxins to gangliosides, or they may act before internalization to prevent internalization or they could be inhibitors which would stop the catalytic action by blocking the active site or by chelating the active-site zinc.

In an attempt to identify suitable small-molecule ligands that bind to the C-fragment of clostridium tetanus neurotoxin (TeNT), several small molecules were screened by computational chemistry and then tested with modeling, docking and electrospray ionization mass spectroscopy (ESI-MS) (Lightstone *et al.*, 2000). Of the many compounds tested, doxorubicin, a DNA-intercalator molecule, was identified to bind with a binding constant of 9.4 μM. Also, from the declustering potential used in ESI-MS, it was concluded that it binds in a hydrophobic pocket. It has been shown that it competes with gangliosides for binding. Here, we present crystallographic evidence for doxorubicin binding to clostridium neurotoxins. We used BoNT/B in our studies since (i) a high-resolution structure was available, (ii)

Table 1
Data and refinement statistics.

Unit-cell parameters (Å,°)	$a = 76.27$, $b = 122.93$, $c = 95.42$, $\beta = 112.95$
Space group	$P2_1$
Resolution range (Å)	50.0–2.5
Total No. of reflections	197506
No. of unique reflections	52722
R_{sym}	6.7 (31.9)
Completeness	99.1 (95.2)
Average $I/\sigma(I)$	14.3
R factor	0.217
R_{free}	0.276
No. of protein atoms	10617
No. of water molecules	354
No. of heterogen atoms	45
Average B factor (Å^2)	
Protein	29.8
Water molecules	27.5
Heterogens	37.8
RMSD	
Bond lengths (Å)	0.007
Bond angles (°)	1.23

all clostridium neurotoxins share significant sequence homology at the C-terminus and (iii) they all possess similar structure (Lacy *et al.*, 1998; Swaminathan & Eswaramoorthy, 2000*b*; Umland *et al.*, 1997).

2. Materials and methods

BoNT/B crystals were obtained as described previously (Swaminathan & Eswaramoorthy, 2000*a*). PEG 4000 was used as precipitant in MES buffer pH 6.0 to grow the crystals. The protein–doxorubicin complex crystals were prepared by soaking BoNT/B crystals in mother liquor containing doxorubicin. The best soaking condition was obtained when crystals were soaked for 36 h in mother liquor containing 50 m*M* doxorubicin.

Data were collected from a crystal at beamline X12C of National Synchrotron Light Source, Brookhaven National Laboratory with the use of a CCD-based detector (Brandeis B1.2). The data collection and processing were performed using *MARMAD* (Skinner & Sweet, 1998) and *HKL/DENZO* (Otwinowski & Minor, 1997). The data-collection statistics are given in Table 1. Crystals of BoNT/B are prone to non-isomorphism even among crystals from the same crystallization well. As the comparison of structure factors of crystals soaked in doxorubicin with those of the native crystal gave an R_{merge} of 0.49, the structure of the complex was determined by the molecular-replacement method using the native structure as a model with *AMoRe* (Navaza & Saludjian, 1997). The model was refined with *CNS* (Brunger *et al.*, 1998) until convergence. The σ-weighted difference Fourier density map was calculated and checked for the possible bound drug. With the available information about the sialyllactose-binding site and the presence of a continuous residual density in the difference density map, the binding site of doxorubucin was identified and the ligand was modeled with the program *O* (Jones *et al.*, 1991). The model was refined after including doxorubicin and 354 water molecules. The final R and R_{free} are 0.22 and 0.28, respectively. The refinement parameters are included in Table 1. The structure was examined with *PROCHECK* (Laskowski *et al.*, 1993) and the coordinates have been submitted to the PDB (PDB code 1i1e). The $2F_o - F_c$ map for doxorubicin is shown in Fig. 1. However, the density is very weak for two terminal atoms which is not unusual as the drug may be disordered at the tail part of the binding.

3. Results and discussion

The botulinum neurotoxin B molecule comprises three structural domains arranged almost linearly, with the translocation domain (HC_N) in the middle flanked by the binding (HC_C) and the catalytic (LC) domains. The catalytic domain and the N-terminal domain of the heavy chain HC_N are held together by a loop (also called the belt region) which is a part of the HC_N domain. The HC_C has minimal interaction with the HC_N domain and is tilted away from the translocation domain. The region between the binding and translocation domains is filled with water molecules, which seems to be a possible interaction site for receptors (Swaminathan & Eswaramoorthy, 2000*b*). The HC_C domain consists of two structural subdomains, a β-sheet/jelly-roll domain and a trefoil domain. The C-terminal half of the HC_C domain contains the binding site for gangliosides.

The ganglioside recognition in TeNT was identified as the carboxy-terminal 34 residues of the C fragment (residues 1282–1315), and the sequence homology among clostridium neurotoxins is very high near the C-terminal region (Shapiro *et al.*, 1997). The photoaffinity labeling occurred predominantly at His1292 of TeNT, which corresponds to Glu1265 of BoNT/B. The gangliosides, especially the 1b series (*e.g.* GT1b or GD1b) showed good affinity for binding to the C-fragment of TeNT. The structures of the binding domains are also very similar in the crystal structures determined so far (Lacy *et al.*, 1998; Swaminathan & Eswaramoorthy, 2000*b*; Umland *et al.*, 1997). In BoNT/A, tryptophan fluorescent quenching is accompanied by ganglioside binding, suggesting that a solvent-exposed tryptophan may be present near the binding site (Kamata *et al.*, 1997). Trp1288 of TeNT or Trp1261 of BoNT/B is present in this C-terminal region and is exposed to the solvent. Crystallographic evidence for a ganglioside-binding site has been shown in the crystal structure of the BoNT/B–sialyllactose complex (Swaminathan & Eswaramoorthy, 2000*b*). The sialic acid of sialyllactose binds in the above-mentioned region and stacks between Trp1261 and His1240 in BoNT/B. However, sialic acid does not make any contact with Glu1265 or residues near Glu1265 in the primary sequence as suggested by biochemical

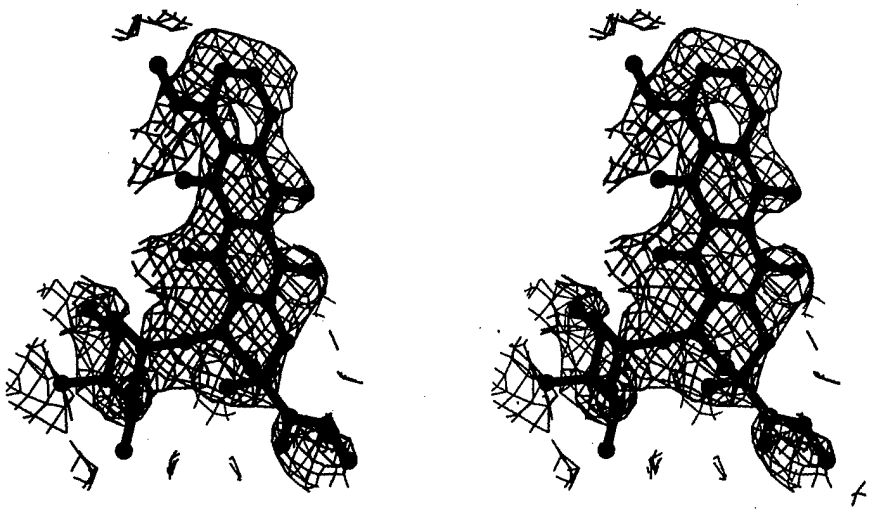

Figure 1
Stereographic view of $2F_o - F_c$ map for doxorubicin. The map is contoured at 1σ. This figure was created with *BOBSCRIPT* and *MOLSCRIPT* (Kraulis, 1991).

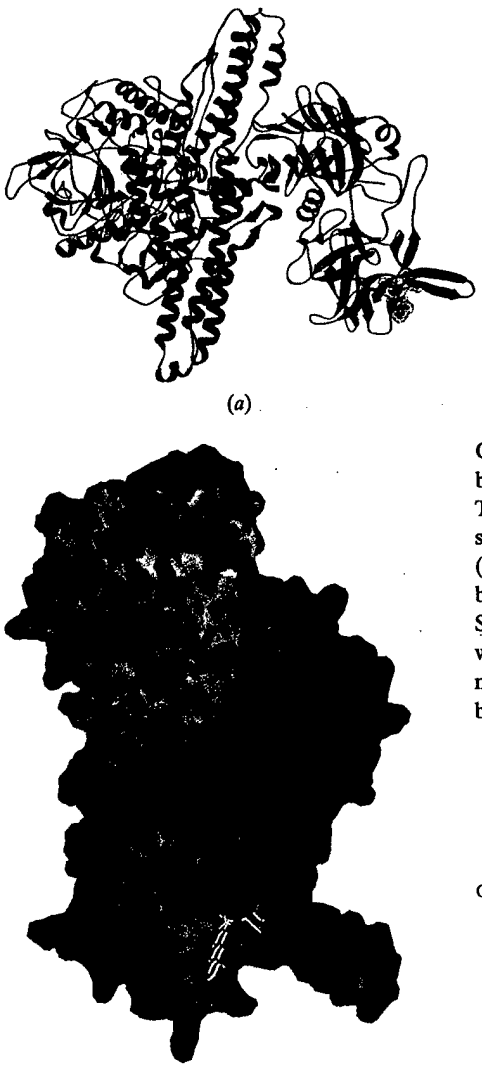

(*a*)

(*b*)

Figure 2
(*a*) *RIBBONS* (Carson, 1991) representation of the intact BoNT/B molecule. The bound doxorubicin molecule is shown as a ball-and-stick model, with the van der Waals surface as a dotted surface. (*b*) *GRASP* (Nicholls *et al.*, 1991) representation of the surface curvature of the C-fragment of BoNT/B with doxorubicin shown as a stick model. The orientation of the molecule is similar to that of (*a*).

studies (Shapiro *et al.*, 1997). A pocket is formed between His1240 and Trp1261 in BoNT/B and this pocket is present in all clostridium neurotoxins for which structures are known. In view of these facts, it may be concluded that this binding site is common to all clostridium neurotoxins.

Doxorubicin (Dox) binds in a cavity formed by residues Glu1188, Glu1189, His1240, Tyr1260 and Trp1261 (Fig. 2). This binding site is the same as that for sialyllactose for BoNT/B and possibly for gangliosides for all clostridium neurotoxins. Doxorubicin interacts with the protein through O13 and O14 of its hydroxy acetyl group, which is buried in the cavity. The numbering scheme of Dox is given in Fig. 3(*a*). His1240 makes a hydrogen bond with Dox and Trp1261 is stacked with the planar aglycone moiety of the Dox, with the D ring facing the solvent region. Most of the O atoms and the N atom in Dox are hydrogen bonded to the protein (Fig. 3*b*). O14 hydrogen bonds with Gly1238 N and Cys1257 O, O13 hydrogen bonds to His1240 N, and O9 and O11 are bonded to His1240 ND1 and Ser1259 OG, respectively. Glu 1188O forms bifurcated hydrogen bonds with O11 and O12 of the doxorubicin. The pyranose ring interacts with a symmetry-related molecule of the protein (Fig. 3*b*). N3*, O4* and O5* are hydrogen bonded with Glu331 OE1, Asp332 O and Ser333 N, respectively. Also, O6 interacts with Glu331 O of the symmetry-related molecule. Table 2 lists the interactions between the neurotoxin and doxorubicin.

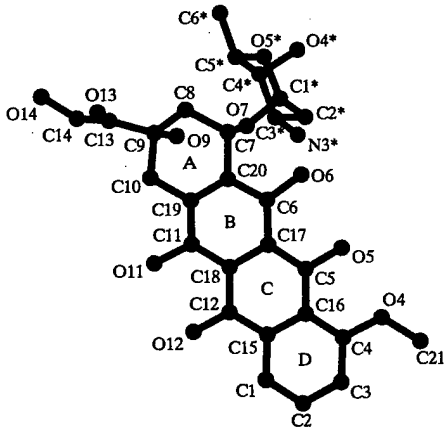

(*a*)

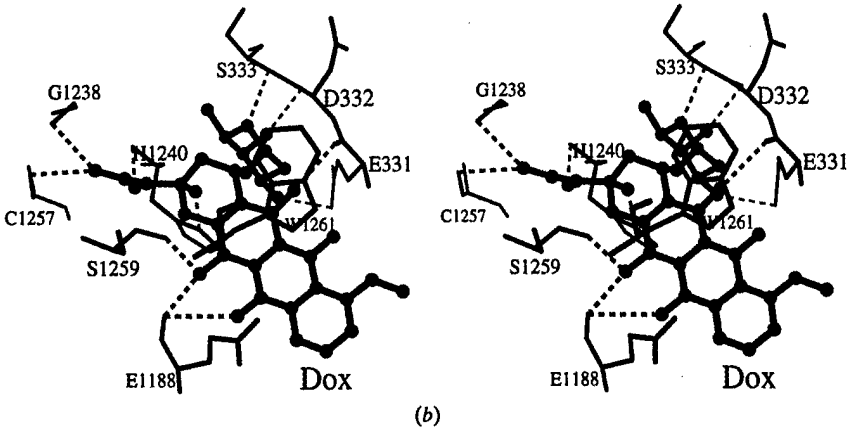

(*b*)

Figure 3
(*a*) The numbering scheme of doxorubicin. (*b*) Stereoview of the interactions of doxorubicin with the protein. Hydrogen-bonding contacts are shown as dashed lines. While amino-acid residues interacting with doxorubicin are shown as a stick model, doxorubicin is shown as a ball-and-stick model.

As there is no antidote available for botulism at present and the preventive measures are also experimental, toxin–potential drug interaction studies are important. The crystal structure of the BoNT/B–sialyllactose complex identified the potential receptor-binding site as the cleft between Trp1261 and His1240 (Swaminathan & Eswaramoorthy, 2000*b*). This binding pocket with a tryptophan exposed to solvent is commonly found in all the BoNTs and TeNT. The present study showed that Dox binds to the same site of sialic acid binding. The hydroxyl O atoms O14 and O13 interact with the protein at the same site as sialyllactose. His1240 and Trp1261 are on either side of Dox as with the sialyllactose. Even though the binding site was predicted by a previous study (Lightstone *et al.*, 2000), the orientation of the molecule seems to be different from that proposed. In particular, the direction in which the amino group points is different; while it is pointing toward the interface of the two subdomains of the C-fragment in the model proposed, it is pointing away from the interface in the crystal structure. This may provide an additional clue in designing molecules for inhibiting neurotoxin binding to the membranes.

The widely used anticancer drugs anthracycline antibiotics, daunomycin and doxorubicin are known to interact with DNA with the aglycone ring intercalating between the base pairs of DNA (Cirilli *et al.*, 1992). In the case of the BoNT/B–doxorubicin complex, the aglycone moiety is stacked with Trp1261. As the activity of the anthracycline antibiotics varies with even a small modification in its structure, more derivatives of these drugs may have to be studied with BoNT/B to find a potential drug.

Table 2
Doxorubicin–protein interactions.

Doxorubicin	Protein	Distance (Å)
O14	Cys1257 O	3.19
O14	Gly1238 N	2.79
O13	His1240 N	3.01
O9	His1240 ND1	2.40
O11	Ser1259 OG	2.79
O11	Glu1188 O	2.67
O12	Glu1188 O	3.28
Symmetry-related molecule		
N3*	Glu331 OE1	3.05
O4*	Asp332 O	2.74
O5*	Ser333 N	2.97
O6	Glu331 O	3.42

4. Conclusions

The present study has defined the interactions between doxorubicin and the neurotoxin. Also, the difference in orientation of doxorubicin from that of the previous studies (Lightstone *et al.*, 2000) underscores the importance of crystallographic study for understanding the interactions of drug molecules with toxins. Even though the affinity of doxorubicin for neurotoxins may not be strong, it certainly presents itself as a strong lead compound since a number of analogues of doxorubicin have already been synthesized and may present better candidates (Cirilli *et al.*, 1992). With the knowledge that doxorubicin competes with gangliosides to bind to the toxin and that the mechanism is similar to the ganglioside binding, it would be a potential lead compound for drug design to treat botulism.

DK was supported by the Veterans Administration Medical Center, Pittsburgh. This research was supported by the Chemical and Biological Non-proliferation Program – NN20 of the US Department of Energy under Prime Contract No. DE-AC02-98CH10886 with the Brookhaven National Laboratory.

References

Adler, M., Nicholson, J. D. & Hackley, B. E. (1998). *FEBS Lett.* **429**, 234–238.
Brunger, A. T., Adams, P. D., Clore, G. M., Delano, W. L., Gros, P., Grosse-Kunstleve, R. W., Jiang, J. S., Kuszewski, J., Nilges, M., Pannu, N. S., Read, R. J., Rice, L. M., Simonson, T. & Warren, G. L. (1998). *Acta Cryst.* D**54**, 905–921.
Carson, M. (1991). *J. Appl. Cryst.* **24**, 958–961.
Cirilli, M., Bachechi, F. & Ughetto, G. (1992). *J. Mol. Biol.* **230**, 878–889.
Jones, T. A., Zou, J., Cowtan, S. & Kjeldgaard, M. (1991). *Acta Cryst.* A**47**, 110–119.
Kamata, Y., Yoshimoto, M. & Kozaki, S. (1997). *Toxicon*, **35**, 1337–1340.
Kraulis, P. J. (1991). *J. Appl. Cryst.* **24**, 946–950.
Lacy, D. B., Tepp, W., Cohen, A. C., DasGupta, B. R. & Stevens, R. C. (1998). *Nature Struct. Biol.* **5**, 898–902.
Laskowski, R. A., MacArthur, M. W., Moss, D. S. & Thornton, J. M. (1993). *J. Appl. Cryst.* **26**, 283–291.
Lightstone, F. C., Prieto, M. C., Singh, A. K., Piqueras, M. C., Whittal, R. M., Knapp, M. S., Balhorn, R. & Roe, D. C. (2000). *Chem. Res. Toxicol.* **13**, 356–362.
Menestrina, G., Schiavo, G. & Montecucco, C. (1994). *Mol. Aspects Med.* **15**, 79–193.
Montecucco, C. (1986). *Trends Biochem. Sci.* **11**, 314–317.
Montecucco, C., Papini, E. & Schiavo, G. (1994). *FEBS Lett.* **346**, 92–98.
Navaza, J. & Saludjian, P. (1997). *Methods Enzymol.* **276**, 581–594.
Nicholls, A., Sharp, K. & Honig, B. (1991). *Proteins*, **11**, 281–296.
Otwinowski, Z. & Minor, W. (1997). *Methods Enzymol.* **276**, 307–326.
Schiavo, G., Matteoli, M. & Montecucco, C. (2000). *Physiol. Rev.* **80**, 717–766.
Schiavo, G., Rossetto, O., Benfenati, F., Poulain, B. & Montecucco, C. (1994). *Ann. NY Acad. Sci.* **710**, 65–75.
Shapiro, R. S., Specht, C. D., Collins, B. E., Woods, A. S., Cotter, R. J. & Schnaar, R. L. (1997). *J. Biol. Chem.* **272**, 30380–30386.
Simpson, L. L. (1986). *Annu. Rev. Pharmacol. Toxicol.* **26**, 427–453.
Skinner, J. M. & Sweet, R. M. (1998). *Acta Cryst.* D**54**, 718–725.
Söllner, T., Whiteheart, S. W., Brunner, M., Erdjument-Bromage, H., Geromanos, S., Tempst, P. & Rothman, J. E. (1993). *Nature (London)*, **362**, 318–324.
Swaminathan, S. & Eswaramoorthy, S. (2000*a*). *Acta Cryst.* D**56**, 1024–1026.
Swaminathan, S. & Eswaramoorthy, S. (2000*b*). *Nature Struct. Biol.* **7**, 693–699.
Umland, T. C., Wingert, L. M., Swaminathan, S., Furey, W. F., Schmidt, J. J. & Sax, M. (1997). *Nature Struct. Biol.* **4**, 788–792.

R46

149

CHARACTERISATION OF RECOMBINANT NEUROTOXIN HEAVY CHAIN FRAGMENTS AND THEIR USE FOR DELIVERY OF THERAPEUTIC AGENTS.

J.M. Sutton, E. Fashola-Stone, O. Chow-Worn, E.R. Evans, & C.C. Shone

Tetanus toxin (TeNT) and the seven botulinum toxin serotypes (BoNTs) make up the clostridial neurotoxin family, which act by blocking neurotransmitter. The BoNTs act primarily at the neuromuscular junction which results in the widespread flaccid paralysis characteristic of botulism. TeNT, in contrast is transported to the central nervous system where it blocks glycine release from inhibitory interneurons. Each neurotoxin consists of a heavy chain (HC; 100kDa) and a light chain (LC; 50kDa) linked by a disulphide bridge. Domains within the C-terminal 50kDa fragment (H_c fragment) of each neurotoxin heavy chain play the primary role in acceptor-binding while the N-terminal 50kDa of the heavy chain (H_N fragment) is involved in translocation of LC into the nerve terminal.
We have characterised a wide range of recombinant HC fragments from both TeNT and BoNT serotypes. H_C domains for TeNT and at least one BoNT serotype have been produced and shown to retain full binding activity on neuronal cells.
Novel hybrid heavy chains have been produced to address some of the problems identified in using native fragments for neuronal delivery. The properties and potential applications of these molecules for delivery of therapeutic agents to nerve cells will be discussed.

Centre for Applied Microbiology and Research, Salisbury, Wilts., SP4 0JG, U.K.

Archives of Pharmacology, Supplement 2 to Vol. 365, June 2002
International Conference 2002, Hannover, Germany June 8-12, 2002

150

STRUCTURE AND ENZYMATIC ACTIVITY OF BOTULINUM NEUROTOXINS

S. Swaminathan[1], S. Eswaramoorthy[1], D. Kumaran[1]

The seven botulinum neurotoxins (BoNT, serotypes A - G), produced by the anaerobic Gram-positive bacterium *Clostridium botulinum*, share significant sequence homology and structural similarity and are highly potent neurotoxins. They all comprise a heavy chain (H, 100 kDa) and a light chain (L, 50 kDa) held together by a disulfide bond. They bind to the presynaptic membrane of the neuronal cells and are internalized by receptor-mediated endocytosis into nerve cells. They are then translocated by energy and pH-dependent mechanism into the cytosol where they attack and cleave their targets, one of the proteins forming SNARE complex responsible for vesicle fusion and docking, and block the release of neurotransmitters thereby causing muscular paralysis and eventual death. Since reduction of interchain disulfide bond is required for catalytic action, we have determined crystal structures of botulinum neurotoxin B in the reduced and unreduced states and also at various pH levels to study the conformational changes, if any. An overview of our structural studies will be presented along with our work on structural analysis of BoNT/B:inhibitor complexes.
The plasticity of the active site and the roles of glutamate 230, arginine 369 and tyrosine 372 of BoNT/B on the catalytic activity will be discussed from the structural point of view.
Research supported by the U.S Army Medical Research Institute of Infectious Diseases and the Chemical and Biological Non-proliferation Program - NN20 of the U.S. Department of Energy under Prime Contract No. DE-AC02-98CH10886 with Brookhaven National Laboratory.

[1]Biology Department, Brookhaven National Laboratory, Upton, NY 11973, USA

151

TREATMENT OF DYSHIDROTIC HAND DERMATITIS WITH INTRADERMAL BOTULINUM TOXIN

Swartling C[2], Lindberg M[2], Anveden I[2], Naver H[1]

Botulinum toxin type A (Btx A) is now widely used prior to surgery in the treatment of severe focal hyperhidrosis. Hyperhidrosis is also an aggravating factor in nearly 40% of patients with dyshidrotic hand eczema.
The aim of this study was to evaluate the effect of intradermal injections of Btx A on dermatitis in patients with vesicular hand dermatitis.
Methods: Ten patients with vesicular dermatitis were treated on one hand with intradermal Btx A (at mean 162 U Botox, Allergan) with the untreated side as a control.
Results: Self-assessment at follow-up 5-6 weeks after injection on a five-grade scale (none, slight, moderate, good, or very good effect) showed that 7 out of 10 patients experienced good or very good effect. A decrease in itching was shown with a visual linear analogue scale (VAS) for itching, with mean 39 % on the treated side compared with an increase by 52 % on the untreated side. These findings were supported by the evaluation of clinical signs. Six of 7 who experienced good or very good effect also had aggravating hand sweating and/or worsening during the summer.
Conclusion: Btx A can be a valuable alternative for patients with treatment-refractory hand eczema of the vesicular type, especially with hyperhidrosis and/or worsening during the summer.

Department of Neuroscience, Neurology[1], and Dpt. of Dermatology[2], Uppsala University Hospital. SE-75185 Uppsala, Sweden

152

SIDE EFFECTS OF INTRADERMAL INJECTIONS OF BOTULINUM A TOXIN IN THE TREATMENT OF PALMAR HYPERHIDROSIS; A NEUROPHYSIOLOGICAL STUDY.

Swartling C[2], Ståhlberg E[3], Färnstrand C[3], Naver H[1]

Focal palmar hyperhidrosis can be effectively abolished by intradermal injections with botulinum toxin. Muscle weakness of finger grip has been reported as a reversible side effect.
The objective of this work was to measure muscular side effects after treatment of palmar hyperhidrosis with botulinum toxin.
Methods: Compound muscle action potential (CMAP) of the abductor pollicis brevis (APB), abductor digiti minimi (ADM) and first dorsal interosseus muscles at supra maximal median or ulnar nerve stimulation at wrist were measured in 37 patients treated with botulinum toxin (Botox, Allergan Pharmaceuticals).
Results: A decrease of CMAMP was found in APB and ADM compared to pre-injection values on average by 74% and 36% respectively at 3 weeks which returned to normal at 37 weeks. Muscle power for finger abduction and finger opposition was also measured and decreased to a lesser extent. Repetitive nerve stimulation and single fiber EMG showed a disturbed neuromuscular transmission.
Comments: With regard to these results one should be careful using higher doses of Botox than the present 0,8mU/cm^2 in treatment of palmar hyperhidrosis and avoid frequent treatments of relapses.

Department of Neuroscience, Neurology[1], Neurophysiology[3] and Dpt of Dermatology[2], Uppsala University Hospital. SE-75185 Uppsala, Sweden

Role of Zinc in Botulinum Neurotoxins — Structural or Catalytic?

S. Swaminathan, S. Eswaramoorthy and D. Kumaran

Brookhaven National Laboratory
Upton, NY 11973
swami@bnl.gov

Clostridium botulinum produces seven distinct serotypes (A – G) of botulinum neurotoxins (BoNTs) which cause botulism leading to flaccid paralysis and eventual death. Botulinum neurotoxins bind to the presynaptic membranes of neuronal cells *via* gangliosides and a second protein receptor, are internalized and then are translocated into the cytosol by a pH dependent mechanism where they attack and cleave one of the three proteins of SNARE complex. This inhibits the formation of SNARE complex which is required for vesicle docking and fusion and hence blocks neurotransmitter release causing flaccid paralysis. Though they cleave specific substrates at specific peptide bonds, they all contain a zinc-binding motif (HExxH) and are classified as zinc endopeptidase. The role of zinc has been investigated by biochemical methods and the presumed structural changes caused by the removal of zinc have been analyzed by spectroscopic methods but no x-ray structure is available on zinc-depleted toxin, so far. Apo toxin crystals were prepared either by titrating the pH in the crystal or by treatment with EDTA before crystallization. Results from these two studies will be presented.

Research supported by the Chemical and Biological Non-proliferation program - NN20 of the U.S. Department of Energy and the U.S. Army Medical Research Acquisition Activity (Award No. DAMD17-02-2-0011) under prime contract No. DE-AC02-98CHI0886 with Brookhaven National Laboratory.